Theoretical Determination of the Efficiency of Aerosol Particle Collection by Falling Columnar Ice Crystals

N. L. MILLER AND P. K. WANG

Department of Meteorology, University of Wisconsin, Madison, Wisconsin

(Manuscript received 16 February 1988, in final form 18 October 1988)

ABSTRACT

A theoretical model for the removal of aerosol particles by falling columnar ice crystals which incorporates gravitational, inertial, thermophoretic, diffusiophoretic, and electrostatic mechanisms has been formulated. The results of this trajectory model, combined with earlier results, determine the collection efficiency for submicron particles as a flux onto a collector surface for any geometry and due to Brownian diffusion, thermo- and diffusiophoresis, as well as electrostatic forcing. The combination of these two models provides scavenging efficiencies for aerosol particles of radii $0.001 \leqslant r \leqslant 10.0$ μm by columnar ice crystals with associated Reynolds numbers ranging from 0.5 to 20.0. This quantitative study indicates the effect of particle size, charge, and atmospheric conditions.

1. Introduction

Field (Starr and Mason 1966; Carnuth 1967; Graedel and Franey 1975; Magono et al. 1975), laboratory (Sood and Jackson 1970; Knutson et al. 1976), and theoretical (Greenfield 1957; Slinn and Hales 1970, 1971; Pilat and Prem 1976, 1977; Grover et al. 1977; Wang et al. 1978; Wang 1985; Wang and Pruppacher 1980; Martin et al. 1980) studies have indicated that precipitation processes play a major role in the removal of suspended aerosol particles from the atmosphere. Field investigations made by Carnuth (1967), Graedel and Franey (1975) and Magono et al. (1975) have indicated that falling ice crystals may remove up to fifty times more efficiently than the equivalent liquid water content of falling raindrops. So far, field and laboratory studies have difficulty resolving detailed quantitative relationships among scavenging mechanisms; however, theoretical models verified by experimental and other theoretical results can be used.

Quantitative studies of the scavenging mechanisms and the interdependence on atmospheric variables for aerosol particles of radii $0.001 \leqslant r \leqslant 10.0$ μm were initiated by Greenfield (1957) who performed the calculation of raindrop-AP scavenging efficiencies. Since then many theoretical studies (e.g., Slinn and Hales 1970, 1971; Slinn 1980; Pilat and Prem 1976, 1977; Grover et al. 1977; Wang et al. 1978; Wang and Pruppacher 1980; Wang 1983a; among others) as well as experimental studies (Beard and Grover 1974; Wang and Pruppacher 1977; Lai et al. 1978; Leong et al.

1982) were carried out. Many of these theoretical models produced results that agree closely with experimental values. The problem of drop–aerosol scavenging is therefore relatively well understood. In contrast, the scavenging of aerosol particles by ice crystals is not as adequately studied.

Recently a few investigations started to carry out some theoretical studies of the ice scavenging phenomenon (Wang and Pruppacher 1980; Martin et al. 1980a,b; Wang 1985). Martin et al. dealt with planar ice crystals and provided collection efficiencies for aerosol radii from 0.001 to 10.0 μm. Wang and Pruppacher (1980) treated the scavenging of aerosol particles of radii 0.5 μm or less by columnar ice crystals. This and Wang's (1985) model are essentially flux models in which the effect of inertial impaction was not included. Since columnar shape is one of the two basic shapes of ice crystals in the atmosphere and indeed there are many columnar ice crystals in cirrus clouds, it is felt necessary to determine the columnar ice crystal–aerosol particle scavenging efficiencies for the entire aerosol size range.

Motivated by the aforementioned need, a new collection efficiency model has been formulated for the removal of aerosol particles by falling columnar ice crystals. This model incorporates computed numerical solutions for velocity, water vapor, and temperature fields around seven isolated columnar ice crystals. This paper discusses the theory and results of this model coupled to the flux model of Wang (1985).

2. The mathematical model

The present model extends the method of determining drop-aerosol particle collection efficiency as

Corresponding author address: Dr. Pao K. Wang, Dept. of Meteorology, University of Wisconsin—Madison, 1225 W. Dayton Street, Madison, Wisconsin 53706.

given in Wang et al. (1978) to the columnar ice crystal–aerosol particle scavenging problem. Two complementary models which compute collision efficiencies by columnar ice crystals have been formulated: 1) a trajectory model for aerosol particles 0.5 μm and larger and 2) a flux model for aerosol particles 0.5 μm and smaller. The combined trajectory and flux models yield the collection efficiencies of aerosol particles of radii 0.001 to 10.0 μm by columnar ice crystals.

a. The trajectory model

Particle trajectory models are based on Newton's second law of motion. The aerosol particle position relative to the columnar ice crystals, $\mathbf{R}(t)$, is obtained from the equation of motion:

$$\frac{d^2\mathbf{R}(t)}{dt^2} = \frac{1}{m_p}[\mathbf{F}_g + \mathbf{F}_d\mathbf{F}_e + \mathbf{F}_{th} + \mathbf{F}_{df}] \qquad (1)$$

where m_p is the mass of the aerosol particle, $\mathbf{F}_g$ is the buoyancy corrected gravitational force:

$$\mathbf{F}_g = m_p\mathbf{g}(\rho_p - \rho_a)/\rho_p \qquad (2)$$

where $\mathbf{g}$ is the gravitational acceleration, ρ_p is the bulk density of the particle, and ρ_a the air density.

The drag force of the flow on the aerosol particle is

$$\mathbf{F}_d = -6\pi\eta_a r_p(\mathbf{v}_p - \mathbf{u})/C_{sc} \qquad (3)$$

where η_a is the dynamic viscosity of the air, r_p the aerosol radius, $\mathbf{v}_p$ ($= d\mathbf{R}/dt$) is the velocity of the aerosol particle, and $\mathbf{u}$ the air velocity. The Stokes–Cunningham slip correction factor, C_{sc}, has been defined by Junge (1963) as $C_{sc} = 1.0 + \alpha N_{kn}$, where $\alpha = 1.26 + 0.40 \exp(-1.1/N_{kn})$. The Knudsen number $N_{kn} = \lambda/r_p$ where λ is the mean free path of the air molecules.

The air flow velocity, $\mathbf{u}$, is obtained by solving the Navier–Stokes equations based on the techniques of Hamielec and Raal (1969), LeClair et al. (1970), and Schlamp et al. (1975). The flow past a columnar ice crystal is approximated by the flow past an infinite circular cylinder having the same radius and same terminal fall velocity. The seven cases calculated here (N_{Re} = 0.5, 0.7, 1.0, 2.0, 5.0, 10.0, 20.0) are the same as those done by Schlamp et al. (1975) and the results agree very well with theirs also.

The electrostatic force, $\mathbf{F}_e$, on a particle near a charged columnar ice crystal is

$$\mathbf{F}_e = Q_p\mathbf{E}_c. \qquad (4)$$

Takahashi (1973) has shown that the particle point charge may be represented as $Q_p = qr_p^2$ where the constant q ranges from 0.2 to 2 esu cm^{-2}, the latter being the mean charge values in the thunderstorm condition. The electric field around a long cylinder, $\mathbf{E} = -\nabla\varphi_e$, where φ_e is the electric potential, has been given by Smythe (1968);

$$\mathbf{E}_c = 2Q_{c/l}\mathbf{e}_r/R(t) \qquad (5)$$

where $\mathbf{e}_r$ is the unit vector in the radial direction and $Q_{c/l} = qr_c^2$ is the charge per unit length of cylinder of radius r_c.

Thermophoretic force, $\mathbf{F}_{th}$, arises from a temperature gradient, ∇T, and is given by Brock (1962) as

$$\mathbf{F}_{th} = C_{th}\nabla T \qquad (6)$$

where

$$C_{th} = -12\pi\eta_a r_p(k_a + 2.5k_p N_{kn})k_a/$$
$$[5(1 + 3N_{kn})(k_p + 2k_a + 5k_p N_{kn})P] \qquad (7)$$

and k_a and k_p are the thermal conductivity of the air and aerosol particle and P is the air pressure.

A diffusiophoretic force, $\mathbf{F}_{df}$, is created by a flux of water vapor and is given by Hidy and Brock (1970) as

$$\mathbf{F}_{df} = C_{df}\nabla\rho_v \qquad (8)$$

where

$$C_{df} = 6\pi\eta_a r(0.74 D_{va}M_a)/[(1 + \alpha N_{kn})M_w\rho_a] \qquad (9)$$

ρ_v and ρ_a are the density of water vapor and air, and M_w and M_a are the molecular weights of water and air; D_{va} is the diffusivity of water vapor in air.

The temperature and water vapor density fields are computed as the solutions to the temperature and vapor density convective-diffusion equations for each ice crystal, based on techniques given in Woo (1971). Computed angular dependent Nusselt number [Nu(Θ) $= -[\partial\eta_T/\partial r]_s$, $\eta_T = (T - T_\infty)/(T_s - T_s)$, s is the ice crystal surface] and Sherwood number [Sh(Θ) $= -[\partial\eta_\rho/\partial r]_s = (\rho_v - \rho_{v,\infty})/(\rho_{v,s} - \rho_{v,\infty})$] indicate temperature and water vapor density gradients at the ice crystal surface. These computed values agree with those in the literature (Dennis and Chang 1969; Woo 1971).

Collision efficiencies of aerosol particles greater than 0.5 μm are determined by the trajectory model if the particle fields do not affect the ice crystals velocity, water vapor, and temperature fields. This is justified by requiring that r_p/r_c is less than 0.5 (Grover 1980). The collision efficiency by ice crystal via the trajectory model is defined as

$$E_t = y_c/(r_p + r_c) \qquad (10)$$

where y_c is the maximum initial horizontal offset from the vertical axis which yields a trajectory that just grazes the ice crystal. The ice crystal is assumed to fall with longer dimension in the horizontal direction. This linear collision efficiency is the same as that used by Schlamp et al. (1975) and is also equivalent to the one defined in Wang (1983b). The latter point can be easily understood if both the numerator and denominator are multiplied by the length of the ice crystal, L. The numerator then becomes the effective kernel K and the denominator becomes the geometrical kernel K^*, and

Eq. (10) is then formally equivalent to the collision efficiency defined in Wang (1983b).

Grazing collisions can occur as front and rear captures. Rear captures occur when there are eddies present ($R_e > 8.5$ for cylinders) or when electrostatic, thermophoretic, or diffusiophoretic forces exhibit an attractive force on the rear half of the ice crystal, causing a collision to occur. When eddies are present, a collision is said to occur once an AP is trapped in a circulating eddy in the wake of the ice crystal. The value for y_c is found by choosing an initial offset value, $y_i = (y_1 + y_h)/2$ (y_1 is initially zero, y_h is initially 2.5 ice crystal radii), and integrating in time for the resultant trajectory. The initial trajectory is chosen always to miss; the following offset is determined by bisecting the offset value, i.e., for a miss $y_h = y_i$, for a hit $y_1 = y_i$, i is the particular iteration. A grazing collision occurs when $(y_h - y_1)/y_i < \epsilon_c$; then $y_c = y_i$. For these calculations the collision tolerance $\epsilon_c = 10^{-4}$.

b. The flux model

An analytical flux model for the convective diffusion of aerosol particles less than 0.5 μm by ice crystals of arbitrary shapes has been formulated by Wang (1985). This model considers Brownian diffusion as well as electrostatic, thermophoretic, and diffusiophoretic forcing. Effects due to gravity are negligible in this size range. The flux density of aerosol particles is given as

$$\mathbf{j}_p = n\mathbf{V}_{\text{drift}} - \bar{f}_p D_B \nabla n \qquad (11)$$

where n is the particle concentration. The drift velocity is defined as

$$\mathbf{V}_{\text{drift}} = B(\mathbf{F}_e + \bar{f}_h \mathbf{F}_{th} + \bar{f}_v \mathbf{F}_{df}). \qquad (12)$$

The mobility is defined as $B = C_{\text{sc}}/(6\pi\eta_a r_p)$ and the Brownian diffusion coefficient as $D_B = Bk_bT$, k_b is the Boltzmann constant. The thermal and vapor ventilation factors, $\bar{f}_h$ and $\bar{f}_v$, are calculated using the empirical formulas of Hall and Pruppacher (1977) and the Brownian ventilation factor $\bar{f}_p$ is determined by the same formulas as $\bar{f}_v$ except the Brownian diffusion coefficient D_B replaces the water vapor diffusivity D_v. Steady-state conditions result in the conservation of particle concentration, $\nabla \cdot \mathbf{j}_p = 0$. The assumption that the forces are nondivergent and conservative leads to the steady-state ventilation enhanced convective-diffusion equation,

$$\mathbf{V}_{\text{drift}} \cdot \nabla n - \bar{f}_p D_B \nabla^2 n = 0. \qquad (13)$$

The boundary conditions to Eq. (13) are

$n = 0$ at the ice crystal surface

$n = n_\infty$ far away from the ice crystal.   (14)

To solve Eq. (13) the forces are expressed as gradients of potentials. The electrostatic, temperature, and vapor density fields can be described by Laplace equations

$$\nabla^2 \varphi_e = 0 \qquad (15a)$$

$$\nabla^2 T = 0 \qquad (15b)$$

$$\nabla^2 \rho_v = 0. \qquad (15c)$$

Based on (15), a scalar force potential, φ_f, can be defined:

$$\nabla \varphi_f = \mathbf{F}_e + \mathbf{F}_{th} + \mathbf{F}_{df} \qquad (16a)$$

where

$$\mathbf{F}_e = C_e \nabla \varphi_e, \quad C_e = -Q_p \qquad (16b)$$

$$\mathbf{F}_{th} = C_e \nabla T \qquad (16c)$$

$$\mathbf{F}_{df} = C_{df} \nabla \rho_v \qquad (16d)$$

and Eq. (16a) satisfies the Laplace equation,

$$\nabla^2 \varphi_f = 0. \qquad (17)$$

The solution to Eq. (13) satisfying Eqs. (14) and (17) is given by (Wang 1983a)

$$n = n_\infty \{ \exp[B(\varphi_{f0} - \varphi_f)/\bar{f}_p D_B] - 1 \}/$$
$$[\exp(B\varphi_{f0}/\bar{f}_p D_B) - 1], \qquad (18)$$

where

$$\varphi_{f0} = C_e/C_c + \bar{f}_h C_{th}(T_\infty - T_s)$$
$$+ \bar{f}_v C_{df} C_{df}(\rho_{v,\infty} - \rho_{v,s}) \qquad (19)$$

is the total force potential at the surface of the ice crystal and C_c is the capacitance for a columnar cylinder. The force potential φ_f is set to 0 at the infinity. The resulting collision kernel for a particle flux is

$$K_f = -\frac{1}{n_\infty} \oint_s \bar{f}_p D_p (\nabla n) ds$$
$$= -4\pi B_{f0} C_c/[\exp(B\varphi_{f0}/\bar{f}_p D_B) - 1]. \qquad (20)$$

In the above derivation, the hydrodynamic effect and its coupling with other forces are taken care of by the overall ventilation factors. The collection efficiency is defined as

$$E_f = K_f / K^* \qquad (21)$$

where $K^* = A_c V_\infty$ for submicron aerosols. The ice crystal cross-sectional area perpendicular to the fall direction is A_c and the terminal velocity is V_∞.

Collection efficiencies are equivalent to collision efficiencies if it is assumed that there is no rebound of particles from the ice crystal surface when there has been a collision.

3. Methods of evaluation

Solutions to Eqs. (10) and (20) were computed for seven columnar ice crystals with Reynolds numbers, radii, lengths, densities and terminal velocities as listed

in Table 1. The results presented here correspond to an atmospheric pressure of 600 mb and an ambient temperature of $-20°C$ unless otherwise noted. Values for $\rho_a(T)$ are from the Smithsonian Meteorological Tables. Values for $k_a(T) = (5.69 + 0.017T°C) \times 10^{-5}$, $k_p(T) = (3.78 + 0.020T) \times 10^{-5}$, $\lambda(P, T) = 6.6 \times 10^{-6}$ cm $(1013.15 \text{ mb}/P)(T/293.15 \text{ K})$, $D_{va}(P, T) = 0.211(T/273.15 \text{ K})1.94(1013.25 \text{ mb}/P)$, and $\eta_a(T) = (1.718 + 0.0049T - 1.2 \times 10^{-5}T^2) \times 10^{-4}$, $T(°C) < 0$, are from Pruppacher and Klett (1978). The bulk density of the columnar ice crystals and the aerosol particles are 0.6 and 2.0 g cm^{-3} respectively, unless otherwise noted.

4. Results and discussion

Figure 1 indicates collection efficiencies of particles $0.001 \leqslant r_p \leqslant 10.0 \mu m$ by columnar ice crystals with $0.5 \leqslant N_{Re} \leqslant 20.0$. The relative humidity is 95% with respect to ice. (All relative humidities present here are with respect to ice.) It is seen that particles less than $0.9 \mu m$ have increasing collision efficiencies for decreasing N_{Re}. Particles greater than $2.0 \mu m$ exhibit the opposite behavior. The increase in efficiency for decreasing N_{Re} for $r_p < 0.5 \mu m$ is due to the fact that Brownian diffusion is more effective the smaller the collector. The observed increase in efficiency for increasing N_{Re} for $r_p > 2.0 \mu m$ is due to the increased contribution from the inertia term. In this case, as N_{Re} increases, the corresponding flow velocity, u, increases and the value $(u - v_d)$ in F_d also increases.

Figures 2a–g indicate the collection efficiencies at $0.5 \leqslant N_{Re} \leqslant 20.0$ for aerosol particles of $0.001 \leqslant r_p \leqslant 10.0 \mu m$ with different relative humidities: curve 1) 95%; 2) 75%; and 3) 50%, without (solid curve) and with (dotted curve) charge (with "e" label). In these figures, gravitational, inertial, electrostatic, thermophoretic and diffusiophoretic forces as well as Brownian diffusion are present. Through choice of the three humidities, the temperature and water vapor dependence of the thermo- and diffusiophoretic forcing mechanism is highlighted in these figures. It is seen that phoretic forcing occurs in subsaturated air for particles of $0.01 \leqslant r_p \leqslant 2.5 \mu m$. The magnitude of this forcing increases with decreasing relative humidity and for decreasing N_{Re}. It should be noted that thermophoresis is toward
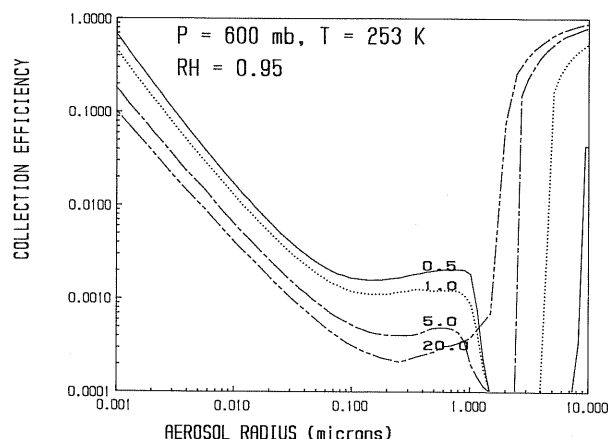

FIG. 1. Variation of collection efficiency for aerosol particles by columnar ice crystals of various Reynolds numbers at 600 mb, 253 K.

the ice crystal surface when it is cooler than the ambient surroundings, while diffusiophoresis acts outward from the crystal surface under the same condition (this is the case for a falling columnar ice crystal). When r_p is less than $1.0 \mu m$, $\mathbf{F}_{th}$ is greater than $\mathbf{F}_{df}$; while for r_p greater than $1.0 \mu m$, $\mathbf{F}_{th}$ is less than $\mathbf{F}_{df}$. The greatest net inward phoretic forcing ($\mathbf{F}_{th} + \mathbf{F}_{df}$) is seen to occur for particles slightly less than $1.0 \mu m$.

The effect of electric charges is shown as lines labeled with (e) after the curve number. In each case $q = 2$ esu cm^{-2}, which corresponds to measured electrostatic charge on drops in a thunderstorm (Takahashi 1973). The presence of electrostatic charges is seen to increase the collection efficiency for high relative humidities and only slightly raise the efficiency for low relative humidities, where the efficiency is already quite high in comparison to the high relative humidity values. The electrostatic effect increases with the square of increasing aerosol particle and ice crystal radii.

The observed zero scavenging zone (ZSZ) within the Greenfield Gap in Fig. 2 occurs as the sum of the radially directed forces, $\mathbf{F}_g + \mathbf{F}_d + \mathbf{F}_{th} + \mathbf{F}_{df}$, approaches zero. Nonzero scavenging values appear as ($\mathbf{F}_{th} + \mathbf{F}_{df}$) is increased in magnitude. As the N_{Re} decreases, the width of the zero scavenging zone increases in the direction of increasing particle size; that is, at 600 mb with 95% relative humidity, for $N_{Re} = 10$ the zero scavenging zone is between 1 and $1.5 \mu m$, for $N_{Re} = 5$ the ZSZ is between 1.5 and $2.5 \mu m$, for $N_{Re} = 1$ the ZSZ is between 1.5 and $4. \mu m$ and for $N_{Re} = 0.5$ the ZSZ is between 1.5 and $7.5 \mu m$.

Figure 3 illustrates the collision efficiency dependence on particle density. Particle density effect is not important for sub $0.5 \mu m$ flux calculations; however, it becomes very significant for supra $0.5 \mu m$ trajectory calculations. In general, increasing particle density increases collision efficiency for $r_p \geqslant 1.5 \mu m$. However, for $r_p < 1.5 \mu m$, the curves are crossing each other, and

TABLE 1. Columnar ice crystal characteristics.

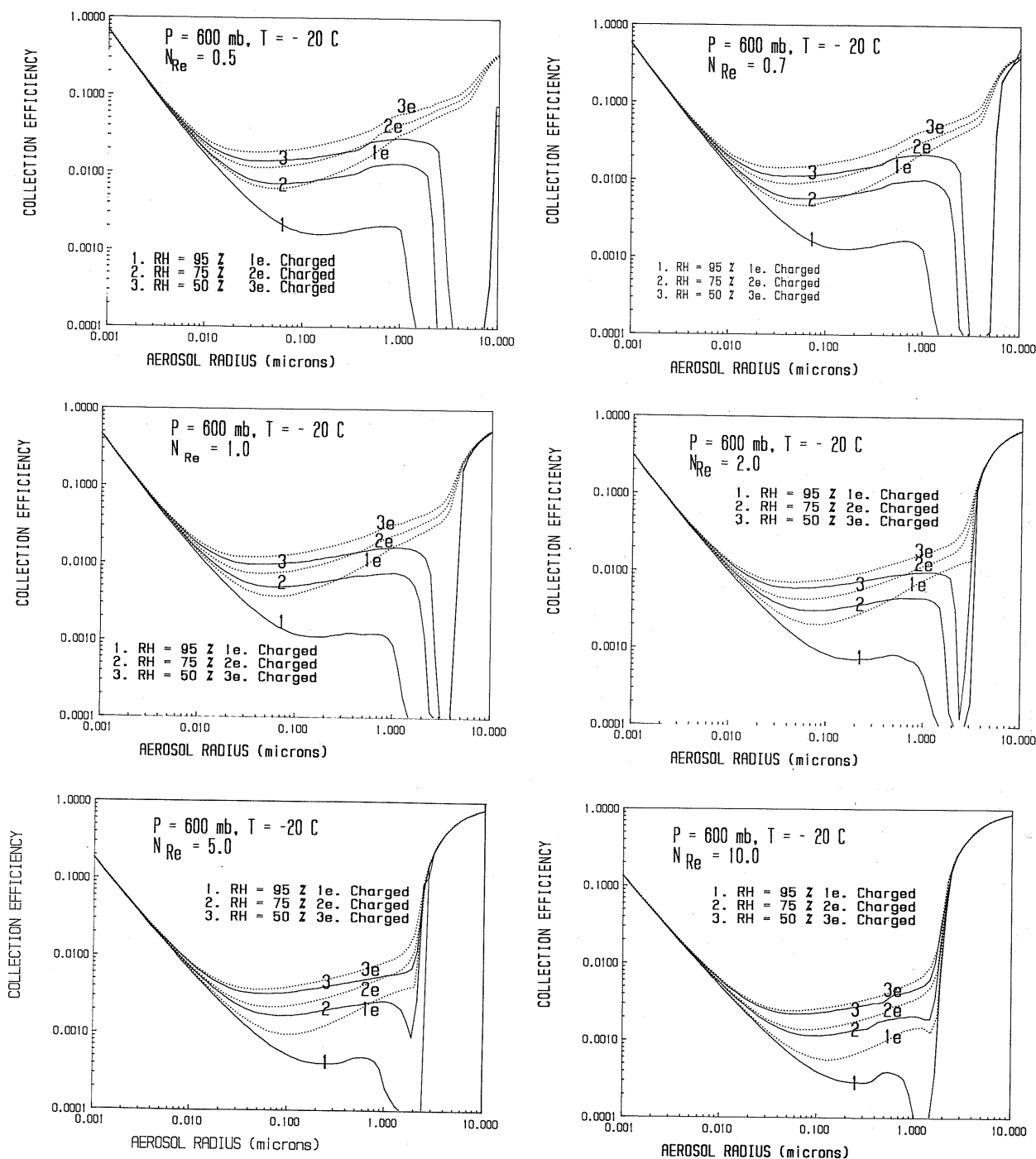| N_{Re}	r_c (μm)	1_c (μm)	ρ_c (g cm^{-3})	V_∞ (cm s^{-1})	$Q_{c/1}$ (esu cm^{-1})
0.5	32.7	93.3	0.6	12.21	-2.139×10^{-5}
0.7	36.6	112.6	0.6	15.26	-2.679×10^{-5}
1.0	41.5	138.3	0.6	19.22	-3.445×10^{-5}
2.0	53.4	237.4	0.6	29.87	-5.703×10^{-5}
5.0	77.2	514.9	0.6	51.65	-1.192×10^{-4}
10.0	106.7	1067.1	0.6	74.76	-2.277×10^{-4}
20.0	146.4	2440.0	0.6	108.98	-4.287×10^{-4}

FIG. 2. Collection efficiency for aerosol particles by columnar ice crystals at 600 mb, 253 K as a function of AP radius. Curves with RH of 1) 95%, 2) 75% and 3) 50% with and without electrostatic charges e) $q = 2$ esu cm^{-2} are presented for (a) $N_{Re} = 0.5$, (b) $N_{Re} = 0.7$, (c) $N_{Re} = 1.0$, (d) $N_{Re} = 2.0$, (e) $N_{Re} = 5.0$, (f) $N_{Re} = 10.0$, and (g) $N_{Re} = 20.0$.

the efficiency decreases with increasing density. Presumably this is due to the weakening inertial effects.

Figure 4 shows the effect of temperature on scavenging efficiency. Increasing temperature increases the efficiency for $r_p < 1.0$ μm. For $r_p > 2.0$ μm the opposite is true. Increasing temperature for minimal phoretic forcing will bridge the zero scavenging zone. Variations in pressure are in the same direction as temperature. This is illustrated in Fig. 5 where the collision efficiency for a columnar ice crystal with $N_{Re} = 10$ is shown for
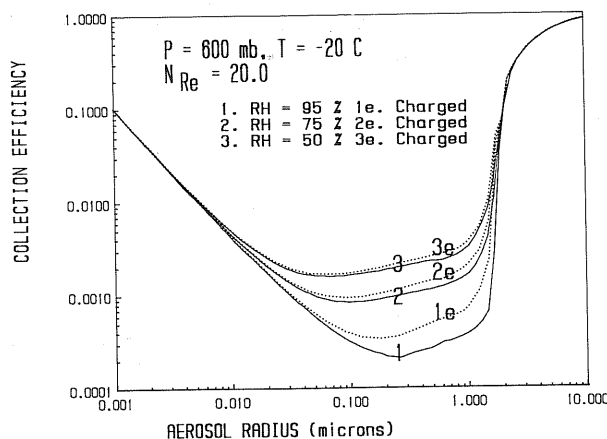
FIG. 2. (*Continued*)

FIG. 4. Collection efficiency of aerosol particles by a columnar ice crystal with $N_{Re} = 10.0$ at 600 mb, 95% relative humidity. Curves represent temperature and electrostatic charge: 1) 253 K, 2) 263 K, 3) 273 K and *e*) $q = 2$ esu cm^{-2}.

several pressure-temperature levels in the atmosphere. Figure 6 shows a comparison of the columnar ice crystal-aerosol scavenging to drop–aerosol scavenging at a 900 mb level. The ice crystal–aerosol results are for a temperature of 268 K while the drop-aerosol results are for 283 K; both are at 95% relative humidity but with respect to ice and with respect to water, respectively. These results, which are plotted as a function of their equivalent geometric kernels K^* (see Wang and Pruppacher 1980, for a discussion of K^*), indicate that columnar ice crystals scavenge more efficiently than drops across the Greenfield Gap except in the region of the zero scavenging zone. This scavenging zone, which is also seen in the drop-aerosol scavenging (Wang et al. 1978), as well as ice plate–aerosol scavenging results (Martin et al. 1980a,b), is wider and occurs over a greater geometric range for columnar ice crystals.

5. Experimental verification of theoretical results

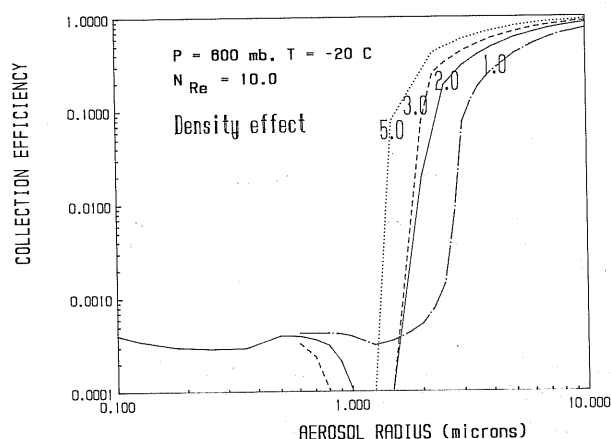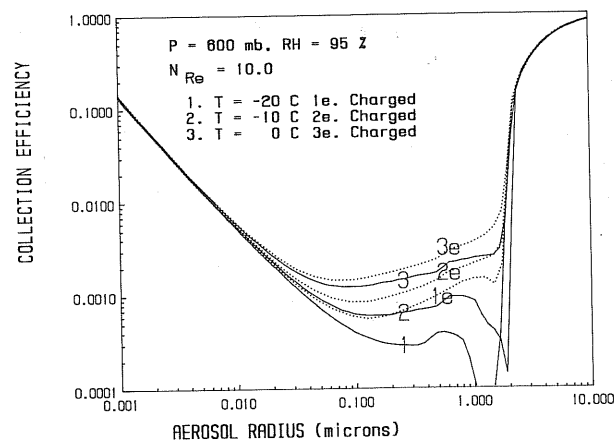Experimental verification of the theory is difficult to obtain. However, a recent experimental study by Sauter

and Wang (1989, accompanying paper in this issue) has yielded efficiency values by columns and needles for aerosol particles of 0.75 μm radii at about 1000 mb and 0°C, and with a relative humidity of 85% with respect to ice. These results are shown in Fig. 7 along with theoretical solutions that correspond to the same atmospheric conditions. It is understood here that due to the many experimental difficulties and nonideal conditions (for example, the crystals are rarely exactly columnar), an exact comparison is not possible. The only parameter that can be used as the basis of comparison is the crystal length. Nevertheless, comparison of theory to experiment for this single particle size and atmospheric conditions shows that they are in the same general magnitude range. Moreover, both show a trend of decreasing efficiency with increasing crystal dimension.
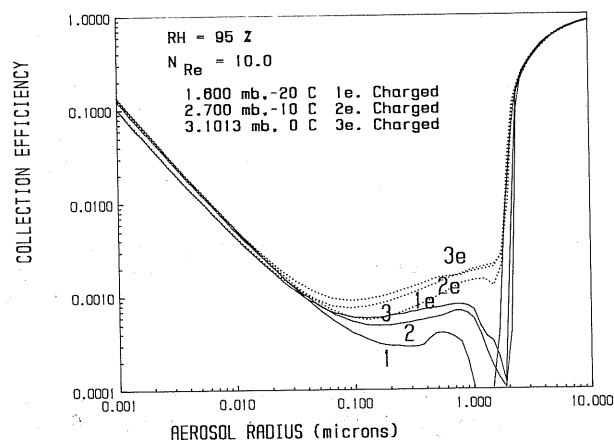

FIG. 3. Collection efficiency as a function of aerosol particle density at 1.0, 2.0, 3.0, and 5.0 gm cm^{-3} at 600 mb, 253 K and 95% RH.

FIG. 5. Collection efficiency as a function of pressure–temperature levels by a columnar ice crystal with $N_{Re} = 10.0$ and 95% RH. 1) 600 mb, 253 K, 2) 700 mb, 263 K, 3) 1013 mb, 273 K.
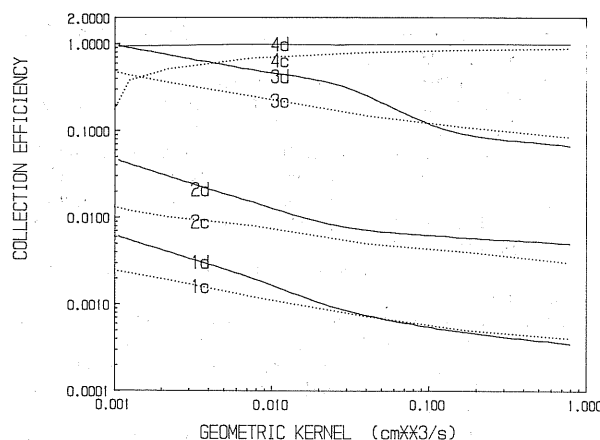
FIG. 6. Comparison of collection efficiencies of aerosol particles by water drops (900 mb, 283 K, solid) and columnar ice crystals (700 mb, 263 K, dotted) for particle radius: 1) 0.1 μm, 2) 0.01 μm, 3) 0.001 μm, 4) 10 μm. Label C represents crystal and label d represents drop. Relative humidity is 95% (see text for explanation).

6. Conclusions

A combined numerical and analytical model that investigates the scavenging efficiencies of aerosol particles by columnar ice crystals has been presented. It was shown that relative humidity, temperature, pressure and electrostatic charge variations can alter the collection efficiency across the Greenfield gap. The foregoing study quantitatively indicates increasing efficiency for decreasing relative humidity and/or increasing temperature, pressure and electrostatic charge. The presence of a zero scavenging zone for flows with $R_e < 20$ was observed for particles 1.5 to 2.0 μm which is seen as a cancellation of radially directed forces. This gap is seen to increase with increasing pressure and with decreasing temperature.
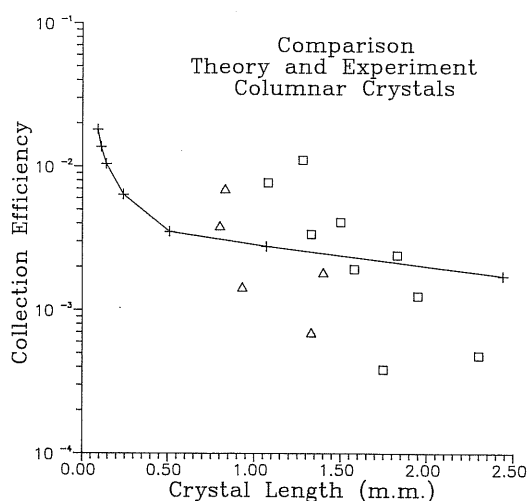

FIG. 7. Comparison of theoretical and experimental results of collection efficiency for aerosol particles by columnar ice crystals. —, Theory; $\triangle$, Needle (exp.); $\square$, Column (exp.).

This is the first quantitative model to indicate the removal of the wide range of particles by columnar ice crystals with accurate velocity, water vapor and temperature fields. Many improvements are possible in the future; for example, calculating the actual three-dimensional fields of flow past finite columns and using them to determine the trajectory. In addition, more experimental studies are definitely needed for verifying the theory.

REFERENCES

Beard, K. V., and S. N. Grover, 1974: Numerical collision efficiencies for small raindrops colliding with micron size particles. *J. Atmos. Sci.*, **31**, 543–550.

Brock, J. R., 1962: On the theory of thermal forces acting on aerosol particles. *J. Colloid Interface Sci.*, **17**, 768–780.

Carnuth, W., 1967: Zur abhaengigheit das aerosol partikel spektrum von meteorogischen vorgaengen and zustaende. *Arch. Meteor., Geophys., Bioklim,* **16A**, 321–343.

Dennis, S. C. R., and G. Z. Chang, 1969: Numerical integration of the Navier-Stokes equations for steady two-dimensional flow. *Phys. Fluid* (Suppl. II), 88–93.

Graedal, T. E., and J. P. Franey, 1975: Field measurements of submicron aerosol washout by snow. *Geophys. Res. Lett.,* **2**, 325.

Greenfield, S., 1957: Rain scavening of radioactive particulate matter from the atmosphere. *J. Meteor.,* **14**, 115–125.

Grover, S. N., 1980: A numerical determination of the efficiency with which aerosol particles collide with cloud and small raindrops. Ph.D. thesis, University of California, Los Angeles.

——, H. R. Pruppacher and A. E. Hamielec, 1977: A numerical determination of the efficiency with which spherical aerosol particles collide with spherical water drops due to inertial impaction, phoretic and electric forces. *J. Atmos. Sci.,* **36**, 1665–1669.

Hall, W. D., and H. R. Pruppacher, 1976: The survival of ice particles falling from cirrus clouds in subsaturated air. *J. Atmos. Sci.,* **33**, 1747–1755.

Hamielec, A. C., and J. D. Raal, 1969: Numerical studies of viscous flow around a circular cylinder. *Phys. Fluids,* **12**, 11–22.

Hidy, G. M., and J. R. Brock, 1970: The dynamics of aerocolloidal systems. *Inter. Reviews in Aerosol Physics and Chemistry,* Vol. 1, Pergamon Press.

Jayaweera, O. K. L. F., and B. J. Mason, 1965: The behaviour of freely falling cylinders and cones in a viscous fluid. *J. Fluid Mech.,* **22**, 709–720.

Junge, C. E., 1963: *Air Chemistry and Radioactivity.* Academic Press, 382 pp.

Knutson, E. O., S. K. Sood and J. D. Stockham, 1976: Aerosol collection by snow and ice crystals. *Atmos. Environ.,* **10**, 395–402.

Lai, K. N., N. Dayan and M. Kerker, 1978: Scavenging of aerosol particles by falling water drops. *J. Atmos. Sci.,* **35**, 674–682.

Le Clair, B. P., A. E. Hamielec and H. R. Pruppacher, 1970: A numerical study of the drag on a sphere at low and intermediate Reynolds numbers. *J. Atmos. Sci.,* **27**, 308–315.

Leong, K. H., K. V. Beard and H. Ochs, 1982: Laboratory measurements of particle capture by evaporating cloud drops. *J. Atmos. Sci.*, **39**, 1130–1140.

Magono, C., T. Endoh and M. Itasaka, 1975: Observation of aerosol particles attached to falling snow crystals. *J. Fac. Sci. Hokkaido University*, **4**, 103–119.

Martin, J. J., P. K. Wang and H. R. Pruppacher, 1980a: A theoretical study of the effect of electric charges on the efficiency with which aerosol particles are collected by ice crystal plates. *J. Colloid Interface Sci.*, **78**, 44–55.

——, —— and ——, 1980b: A theoretical determination of the efficiency with which aerosol particles are collected by simple ice crystal plates. *J. Atmos. Sci.*, **37**, 1628–1638.

——, ——, —— and A. E. Hamielec, 1980: On the efficiency with which aerosol particles of radius larger than 0.1 microns are collected by simple ice crystal plates. *Pure Appl. Geophys.*, **118**, 1109–1129.

Pilat, M. J., and A. Prem, 1976: Calculated particle collection efficiencies of single droplets including inertial impaction, brownian diffusion, diffusiophoresis and thermophoresis. *Atmos. Environ.*, **10**, 13–19.

——, and ——, 1977: Effect of diffusio and thermophoresis on the overall particle collection efficiency of spray droplet scrubbers. *J. Air Poll. Control Assoc.*, **27**, 982–988.

Pitter, R. L., 1978: Influence of electrostatic forces on riming by thin ice plates. *J. Meteor. Soc.*, **56**, 523–526.

——, and H. R. Pruppacher, 1974: A numerical investigation of collision efficiencies of simple ice plates colliding with supercooled drops. *J. Atmos. Sci.*, **31**, 551–559.

——, —— and A. E. Hamielec, 1973: A numerical study of the flow past a thin oblate spheroid at low and intermediate Reynolds numbers. *J. Atmos. Sci.*, **30**, 125–134.

Pruppacher, H. R., and J. D. Klett, 1978: *Microphysics of Clouds and Precipitation.* D. Reidel, 714 pp.

Sauter, D., and P. K. Wang, 1989: An experimental study of the scavenging of aerosol particles by natural snow crystals. *J. Atmos. Sci.*, **46**,

Schlamp, S. N., H. R. Pruppacher and A. E. Hamielec, 1975: A numerical investigation of the efficiency with which simple columnar ice crystals collide with supercooled water drops. *J. Atmos. Sci.*, **32**, 2330–2337.

Slinn, W. G. N., 1980: *Precipitation Scavenging Atmospheric Science and Power Productions, 1979.* D. Randerson, Ed., U.S. Dept. of Energy, Tech. Infor. Center, Oak Ridge.

——, and J. M. Hales, 1970: Phoretic processes in scavenging: *Precipitation Scavenging. AEC Symp. Ser.*, Richland, 411–421.

——, and ——, 1971: A reevaluation of the role of thermo-phoresis as a mechanism of in and below cloud scavening. *J. Atmos. Sci.*, **28**, 1465–1471.

Smythe, W. R., 1968: *Static and Dynamic Electricity.* 3rd ed, McGraw-Hill, 623 pp.

Sood, S. K., and M. R. Jackson, 1969: Scavenging by snow and ice crystals. *Precipitation Scavenging, AEC Symp.*, Richland.

Starr, J. R., and B. J. Mason, 1966: The capture of airborne particles by water drops and simulated snow crystals. *Quart. J. Roy. Meteor. Soc.*, **92**, 490.

Takahashi, T., 1973: Measurement of electric charge on cloud drops, drizzle drops and simulated snow crystals. *Rev. Geophys. Space Phys.*, **11**, 903–924.

Wang, P. K., 1983a: Collection of aerosol particles by a conducting sphere in an external electric field-continuum regime approximation. *J. Colloid Interface Sci.*, **94**, 301–318.

——, 1983b: On the definition of collision efficiency of atmospheric particles. *J. Atmos. Sci.*, **40**, 1051–1052.

——, and H. R. Pruppacher, 1977: An experimental determination of the efficiency with which aerosol particles are collected by water drops in subsaturated air. *J. Atmos. Sci.*, **34**, 1664–1669.

——, and ——, 1980: On the efficiency with which aerosol particles of radius less than 1 μm are collected by columnar ice crystals. *Pure Appl. Geophys.*, **118**, 1090–1108.

——, S. N. Grover and H. R. Pruppacher, 1978: On the effect of electric charges on the scavenging of aerosol particles by cloud and small rain drops. *J. Atmos. Sci.*, **35**, 1735–1743.

Woo, S. D., 1971: Simultaneous free and forced convection around submerged cylinders and spheres. Ph.D. thesis, McMaster University, Hamilton, Canada, 224 pp.

——, and A. E. Hamielec, 1971: A numerical method of determining the rate of evaporation of small water drops falling at terminal velocity in air. *J. Atmos. Sci.*, **28**, 1448.